Quantum kinetic theory of shift-current electron pumping in semiconductors

2000 J. Phys.: Condens. Matter 12 4851

(http://iopscience.iop.org/0953-8984/12/22/317)

J. Phys.: Condens. Matter **12** (2000) 4851–4868. Printed in the UK PII: S0953-8984(00)12367-7

Quantum kinetic theory of shift-current electron pumping in semiconductors

Petr Král†

Department of Physics, University of Toronto, 60 St George Street, Ontario, Toronto, Canada, M5S 1A7

Received 6 March 2000

Abstract. We develop a theory of laser beam generation of *shift currents* in non-centrosymmetric semiconductors. The currents originate when the excited electrons transfer between different bands or scatter inside these bands, and asymmetrically shift their centres of mass in elementary cells. Quantum kinetic equations for hot-carrier distributions and expressions for the induced currents are derived using non-equilibrium Green functions. In applications, we simplify the approach to the Boltzmann limit and use it to model laser-excited GaAs in the presence of longitudinal optical phonon scattering. The shift currents are calculated in a steady-state regime.

1. Introduction

Photovoltaic phenomena in semiconductors can originate in the built-in or induced asymmetry or inhomogeneity of their crystal structures [1]. In non-centrosymmetric (NCS) crystals, different generation rates for carriers at momenta $\pm\boldsymbol{k}$ can be induced by asymmetric electron–hole scattering and other processes. The resulting momentum imbalance generates the so-called *ballistic current*. Recently [2, 3], this momentum asymmetry of carrier generation in semiconductors was achieved by mixing one- and two-photon transitions at frequencies $2\omega_0$ and ω_0, respectively. In reference [4], we describe the effect in GaAs in the presence of scattering on LO phonons. We have also suggested that the current induced by this two-beam coherent control could drive intercalated atoms in carbon nanotubes [5].

In bulk NCS semiconductors, light-induced interband transitions of electrons in reciprocal space are accompanied by their *asymmetrical shifts* in the real space between atoms in elementary cells. Similar shifts occur if the transitions are induced by scattering or in recombination. The first realistic description of analogous effects in magnetic materials was given by Luttinger [6]. The carrier shifts generate the so-called *shift current* [7–10], which has in general three components, excitation $\boldsymbol{J}_e$, scattering $\boldsymbol{J}_s$ and recombination $\boldsymbol{J}_r$, named after the corresponding processes. The carrier transitions and the related currents are symbolically sketched in figure 1(a). The ballistic current and the excitation part of the shift current $\boldsymbol{J}_e$ in GaAs were investigated analytically in reference [11]; $\boldsymbol{J}_e$ induced by transitions between light- and heavy-hole bands was also studied [12]. A summary of older results relating to the shift current is presented in reference [1], but the derivation of the relevant formulae is less clearly documented.

Here, we develop a quantum kinetic theory for the shift current induced by laser excitation and scattering. The expressions for the current components and the transport equations for

† Present address: Department of Chemical Physics, Weizmann Institute of Science, 76100 Rehovot, Israel.

0953-8984/00/224851+18$30.00

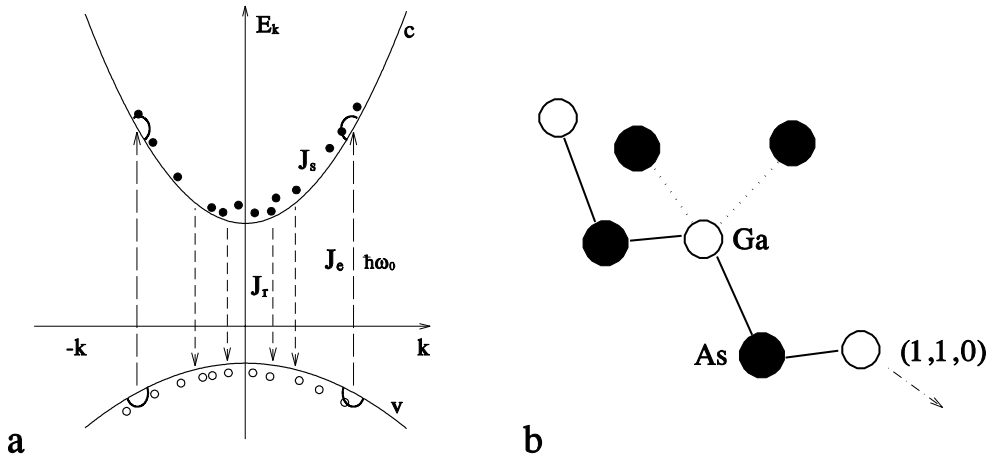

Figure 1. The scheme of the shift-current generation in a NCS semiconductor is shown in panel (a). The current has three components, related to the processes of electron excitation $\boldsymbol{J}_e$, scattering $\boldsymbol{J}_s$ and recombination $\boldsymbol{J}_r$. They result as a consequence of real-space shifts of electrons in the elementary cells that undergo the corresponding transitions in reciprocal space. In panel (b) we show a small section of a zinc-blende structure in GaAs. The excitation conditions and the shift currents $\boldsymbol{J}_{e,s,r}$ generated are described in the text.

carrier populations are derived using non-equilibrium Green functions [13] (NGF). In applications, we simplify the approach to the Boltzmann limit and use it to study optically excited GaAs in the presence of scattering by LO phonons. In our modelling, we consider steady-state excitations by linearly polarized light, and find that $\boldsymbol{J}_e$ is reasonably large, while $\boldsymbol{J}_s$ is two orders smaller and $\boldsymbol{J}_r$ is negligible. Therefore, *continuous electron pumping* through the crystal can be achieved. The ultrafast response of $\boldsymbol{J}_e$, without additional saturation and relaxation tails from $\boldsymbol{J}_s$ and $\boldsymbol{J}_r$, could be useful in optoelectrical applications.

The paper is organized as follows. In section 2 we describe our model system. Section 3 is devoted to the derivation of expressions for the current components. In section 4 these expressions are further approximated. Numerical results for the hot-electron populations and the induced currents in GaAs are presented in section 5.

2. The system studied

The physics of the phenomenon can be understood from figure 1(b), where a segment of the zinc-blende structure for GaAs is shown. The valence band states are predominantly localized around the As atoms, while the conduction band states are shifted toward the Ga atoms. Therefore, if the light is polarized along the $(1, 1, 0)$ direction, the excited electrons transfer from the As atoms at the *bottom* to the Ga atoms in the middle, giving the excitation current $\boldsymbol{J}_e$ in the $(0, 0, -1)$ direction (negative charge). If the light is polarized in the $(1, -1, 0)$ direction, electron transitions along bonds orthogonal to the light polarization, i.e. from the As atoms at the *top* to the Ga atoms in the middle, generate $\boldsymbol{J}_e$ in the $(0, 0, 1)$ direction. During relaxation, the excited electrons (holes) slightly move their centres of charge and stay close to the Ga (As) atoms. Therefore, $\boldsymbol{J}_s$ is rather small, as we show in our calculations. On the other hand, scattering redistributes the carrier momenta, so electrons at Ga atoms recombine symmetrically with holes at all neighbour As atoms, which gives negligible $\boldsymbol{J}_r$.

2.1. The model Hamiltonian

The space shifts of carriers and the related currents can be calculated from a combination of interband and intraband transitions. The length gauge with the elements of the position operator $\boldsymbol{x}$ evaluated as in Blount's work [14, 15] gives a convenient basis for the description [16]. Therefore, we model the photoexcited bulk GaAs by the following Hamiltonian [16]:

$$\begin{aligned} H = \sum_{\alpha;\boldsymbol{k}} \epsilon_\alpha(\boldsymbol{k}) a^\dagger_{\alpha,\boldsymbol{k}} a_{\alpha,\boldsymbol{k}} + \sum_{\boldsymbol{q}} \hbar\omega_{\boldsymbol{q}} b^\dagger_{\boldsymbol{q}} b_{\boldsymbol{q}} \\ - \mathrm{i}e\boldsymbol{E}(t)\cdot\left\{\frac{1}{2}\sum_{\alpha;\boldsymbol{k}}\left(a^\dagger_{\alpha,\boldsymbol{k}}\frac{\partial a_{\alpha,\boldsymbol{k}}}{\partial \boldsymbol{k}} - \frac{\partial a^\dagger_{\alpha,\boldsymbol{k}}}{\partial \boldsymbol{k}} a_{\alpha,\boldsymbol{k}}\right) - \mathrm{i}\sum_{\alpha,\beta;\boldsymbol{k}} \boldsymbol{\xi}_{\alpha\beta}(\boldsymbol{k}) a^\dagger_{\alpha,\boldsymbol{k}} a_{\beta,\boldsymbol{k}}\right\} \\ + \sum_{\alpha,\beta;\boldsymbol{k},\boldsymbol{q}} M_{\alpha\beta}(\boldsymbol{k},\boldsymbol{k}-\boldsymbol{q}) a^\dagger_{\alpha,\boldsymbol{k}} a_{\beta,\boldsymbol{k}-\boldsymbol{q}}(b_{\boldsymbol{q}} + b^\dagger_{-\boldsymbol{q}}) \end{aligned} \tag{1}$$

where coupling to LO phonons is added. Here the creation (annihilation) operators $a^\dagger_{\alpha,\boldsymbol{k}}$ ($a_{\alpha,\boldsymbol{k}}$) describe electrons with the band index α at wave vector $\boldsymbol{k}$ in the Brillouin zone. The operator $b^\dagger_{\boldsymbol{q}}$ ($b_{\boldsymbol{q}}$) creates (annihilates) phonons with the wave vector $\boldsymbol{q}$. The electric field is $\boldsymbol{E}(t) = \boldsymbol{E}_{+\omega_0}(t)\mathrm{e}^{-\mathrm{i}\omega_0 t} + \boldsymbol{E}_{-\omega_0}(t)\mathrm{e}^{+\mathrm{i}\omega_0 t}$, where $\boldsymbol{E}_{+\omega_0}(t) = \boldsymbol{E}^*_{-\omega_0}(t)$ are complex envelope functions. Spins are included in the current by a factor of 2 (see equation (12)).

2.2. The matrix elements

The matrix elements $\boldsymbol{x}_{\alpha\beta}(\boldsymbol{k},\boldsymbol{k}')$ for the position operator are defined as [14]

$$\boldsymbol{x}_{\alpha\beta}(\boldsymbol{k},\boldsymbol{k}') = \mathrm{i}\delta_{\alpha\beta}\frac{\partial}{\partial \boldsymbol{k}}\delta(\boldsymbol{k}-\boldsymbol{k}') + \delta(\boldsymbol{k}-\boldsymbol{k}')\xi_{\alpha\beta}(\boldsymbol{k}) \tag{2}$$

where the functions

$$\xi_{\alpha\beta}(\boldsymbol{k}) = \xi^*_{\beta\alpha}(\boldsymbol{k}) = \int_{\mathrm{U.C.}} \mathrm{d}\boldsymbol{x}\; u^*_{\alpha\boldsymbol{k}}(\boldsymbol{x})\,\mathrm{i}\,\frac{\partial}{\partial \boldsymbol{k}} u_{\beta\boldsymbol{k}}(\boldsymbol{x}) \tag{3}$$

are integrals over the unit cell of the fast components $u_{\alpha\boldsymbol{k}}(\boldsymbol{x})$ in the Bloch wave functions $\psi_{\alpha\boldsymbol{k}}(\boldsymbol{x}) = \mathrm{e}^{\mathrm{i}\boldsymbol{k}\cdot\boldsymbol{x}}u_{\alpha\boldsymbol{k}}(\boldsymbol{x})$. In the following, we use the term $\boldsymbol{r}_{\alpha\beta}(\boldsymbol{k}) = \xi_{\alpha\beta}(\boldsymbol{k})$ for the band off-diagonal elements $\alpha \neq \beta$. They are related to the *interband* velocity elements by

$$\boldsymbol{v}_{\alpha\beta}(\boldsymbol{k}) = \langle\alpha,\boldsymbol{k}|(-\mathrm{i}\hbar/m_e)\boldsymbol{\nabla}|\beta,\boldsymbol{k}\rangle = \frac{\epsilon_\beta(\boldsymbol{k}) - \epsilon_\alpha(\boldsymbol{k})}{\mathrm{i}\hbar}\boldsymbol{r}_{\alpha\beta}(\boldsymbol{k}). \tag{4}$$

The electron–phonon matrix elements [17, 18]

$$M_{\alpha\beta}(\boldsymbol{k},\boldsymbol{k}-\boldsymbol{q}) = M(\boldsymbol{q})\gamma_{\alpha\beta}(\boldsymbol{k},\boldsymbol{k}-\boldsymbol{q}) \qquad \gamma_{\alpha\beta}(\boldsymbol{k},\boldsymbol{k}-\boldsymbol{q}) = \int_{\mathrm{U.C.}} \mathrm{d}\boldsymbol{x}\; u^*_{\alpha\boldsymbol{k}}(\boldsymbol{x})u_{\beta\boldsymbol{k}-\boldsymbol{q}}(\boldsymbol{x}) \tag{5}$$

include the structure factors $\gamma_{\alpha\beta}(\boldsymbol{k},\boldsymbol{k}-\boldsymbol{q})$, which separately depend on the 'incoming' and 'outgoing' momenta $\gamma_{\alpha\beta}(\boldsymbol{k},\boldsymbol{k}-\boldsymbol{q}) \neq f(\boldsymbol{q})$. Therefore, the factor $M(\boldsymbol{q})$ in expression (5) gives the rate of electron scattering, while the real-space shifts of electrons are solely controlled by the lattice [9, 10], determining the factors $\gamma_{\alpha\beta}(\boldsymbol{k},\boldsymbol{k}-\boldsymbol{q})$ (see appendix B). In the approximation of a constant LO phonon energy $\hbar\omega_q \approx \hbar\omega_Q$, the element $M^2(\boldsymbol{q})$ is given by [18]

$$M^2(\boldsymbol{q}) = \frac{M_0^2}{|\boldsymbol{q}|^2} \qquad M_0^2 = 2\pi e^2\hbar\omega_Q\left(\frac{1}{\epsilon_\infty} - \frac{1}{\epsilon_0}\right). \tag{6}$$

The parameters relevant for GaAs are used: $\hbar\omega_Q = 36$ meV, $\epsilon_0 = 12.5$ and $\epsilon_\infty = 10.9$.

3. Description of the system

We describe the problem using non-equilibrium Green functions [19, 20] in the matrix form $G_{\alpha\beta}$, similarly to in reference [4]. The shift current can be expressed through the *interband* elements for NGF, which must be known on a semi-analytical level, so the space shifts can be obtained first by algebraic operations. In older works, the manipulations were carried out in the density matrix formalism, but the intermediate steps were less clearly presented. More recently, NGF were used to investigate the shift current from electron hopping in superlattices [21], and in other photovoltaic phenomena [22, 23].

Here, we develop an approach similar to that of reference [21], and apply it to our system in a steady-state regime. The interband functions $G_{\alpha\beta}$ ($\alpha \neq \beta$) are expressed using the *differential* version of the Kadanoff–Baym equations [19] (KBE) in terms of the intraband $G_{\alpha\alpha}$ from the scattering integrals of these KBE. Then the $G_{\alpha\beta}$ are substituted in the formula for the shift current, where the above-mentioned reordering is performed. Finally, the $G_{\alpha\alpha}$ are calculated numerically from the *integral* version of the KBE [4]. We have not been able to perform this reordering, at least for $\boldsymbol{J}_s$, when $G_{\alpha\beta}$ was expressed using the integral KBE.

3.1. The differential KBE

The differential version of the KBE for the matrix correlation function $\boldsymbol{G}^<$ is [19, 20] ($\chi = (\boldsymbol{k}, t)$; integration over $\bar{\chi}$ is implied)

$$\left(\boldsymbol{G}^{R,0}(\chi, \bar{\chi})\right)^{-1}\boldsymbol{G}^<(\bar{\chi}, \chi') = \left(\boldsymbol{\Sigma}(\chi, \bar{\chi})\boldsymbol{G}(\bar{\chi}, \chi')\right)^< \tag{7}$$

where $(\boldsymbol{G}^{R,0})^{-1} = (G^{R,0}_{\alpha\beta})^{-1}\delta_{\alpha\beta}$ is the inverted free propagator [19]. The 'lesser' operation $<$ can be applied to the functions on the r.h.s. of (7) with the help of the Langreth–Wilkins (LW) rules [24] $(AB)^< = A^<B^A + A^RB^<$. The KBE can be also written in the form where $(\boldsymbol{G}^{A,0})^{-1}$ acts on $\boldsymbol{G}^<$ from the right-hand side, and, in the scattering term, $\boldsymbol{\Sigma}$ is interchanged with $\boldsymbol{G}$.

Subtraction of these two KBE gives [20] ($T = (t + t')/2$)

$$\begin{aligned}\mathrm{i}\hbar\frac{\partial G^<_{\alpha\beta}(\chi, \chi')}{\partial T} &- (\epsilon_\alpha(\boldsymbol{k}) - \epsilon_\beta(\boldsymbol{k}'))G^<_{\alpha\beta}(\chi, \chi') \\ &= \Sigma_{f;\alpha\bar{\gamma}}(\chi, \bar{\chi})G^<_{\bar{\gamma}\beta}(\bar{\chi}, \chi') - G^<_{\alpha\bar{\gamma}}(\chi, \bar{\chi})\Sigma_{f;\bar{\gamma}\beta}(\bar{\chi}, \chi') \\ &\quad + \left(\Sigma_{s;\alpha\bar{\gamma}}(\chi, \bar{\chi})G_{\bar{\gamma}\beta}(\bar{\chi}, \chi')\right)^< - \left(G_{\alpha\bar{\gamma}}(\chi, \bar{\chi})\Sigma_{s;\bar{\gamma}\beta}(\bar{\chi}, \chi')\right)^<.\end{aligned} \tag{8}$$

In the scattering integrals on the r.h.s., field ($\Sigma_{f;\alpha\beta}$) and scattering ($\Sigma_{s;\alpha\beta}$) self-energy functions are introduced [4]. The terms do *not* commute because of the time, momentum and band indices. The momentum and band non-commutativity ultimately leads to the shift currents. The time issue should be less serious, if pulse fields with slow envelope functions are applied to the system, so that gradient expansions in terms of the difference time τ can be performed around the CMS time coordinate T [19, 25]. We adopt this approach here and include only the zero-order terms.

3.2. The self-energy functions

In order to obtain the field self-energy $\Sigma_{f;\alpha\beta}$ for the Hamiltonian (1) in the length gauge, it is necessary to perturbatively expand the Green functions in terms of the light excitation, similarly to in reference [4]. Direct calculation gives

$$\Sigma_{f;\alpha\beta}(\boldsymbol{k}, \boldsymbol{k}', t, t') = -\mathrm{i}e\delta(t - t')\delta(\boldsymbol{k} - \boldsymbol{k}')\boldsymbol{E}(t)\cdot\left\{\frac{1}{2}\left(\frac{\partial}{\partial\boldsymbol{k}'} - \frac{\partial}{\partial\boldsymbol{k}}\right)\delta_{\alpha\beta} - \mathrm{i}\xi_{\alpha\beta}(\boldsymbol{k})\right\} \tag{9}$$

which has zero correlation parts $\Sigma^{<,>}_{f;\alpha\beta}(\boldsymbol{k},\boldsymbol{k}',t,t')=0$. This self-energy acts as an operator, due to the presence of derivatives. When surrounded by functions with two momenta variables, it differentiates the function in front (behind) over $\boldsymbol{k}$ ($\boldsymbol{k}'$), and sets $\boldsymbol{k}=\boldsymbol{k}'$. The derivatives can be shifted from one side to the other side by a partial integration, which changes their signs and combines the two with a prefactor 1. We can also introduce its steady-state form

$$\Sigma^{\pm}_{f;\alpha\beta}(\boldsymbol{k},\boldsymbol{k}')=-\mathrm{i}e\delta(\boldsymbol{k}-\boldsymbol{k}')\boldsymbol{E}_{\pm\omega_0}\cdot\left\{\frac{1}{2}\left(\frac{\partial}{\partial\boldsymbol{k}'}-\frac{\partial}{\partial\boldsymbol{k}}\right)\delta_{\alpha\beta}-\mathrm{i}\xi_{\alpha\beta}(\boldsymbol{k})\right\} \tag{10}$$

which can be obtained by a Fourier transformation of the Dyson equation in the frequency domain [19]. The frequency arguments of the Green functions following $\Sigma^{\pm}_{f;\alpha\beta}$ are shifted by $\mp\omega_0$ (see reference [4]).

Finally, we have to write down the correlation function for the electron–phonon self-energy, which we use in the self-consistent Born approximation:

$$\Sigma^{<}_{s;\alpha\beta}(\boldsymbol{k},\boldsymbol{k}',t,t')=M_{\alpha\gamma}(\boldsymbol{k},\boldsymbol{k}-\bar{\boldsymbol{q}})M_{\delta\beta}(\boldsymbol{k}'-\bar{\boldsymbol{q}},\boldsymbol{k}')G^{<}_{\gamma\delta}(\boldsymbol{k}-\bar{\boldsymbol{q}},\boldsymbol{k}'-\bar{\boldsymbol{q}},t,t')D^{<}(\bar{\boldsymbol{q}},t,t'). \tag{11}$$

Here, the non-locality in momentum and time as well as all kinds of interband transitions are included (summation over $\bar{\boldsymbol{q}}$ and repeated band indices).

3.3. The total shift-current density $\boldsymbol{J}$

The shift-current density $\boldsymbol{J}$ can be expressed in terms of the *interband* velocity elements $\boldsymbol{v}_{\beta\alpha}(\boldsymbol{k})$ and the $\boldsymbol{k}$-diagonal elements of the correlation functions $G^{<}_{\alpha\beta}(\boldsymbol{k},\boldsymbol{k})$. If the perturbing electric field is homogeneous in real space, i.e. invariant with respect to the lattice translation of the crystal, then we would naturally expect these functions to be $\boldsymbol{k}$-diagonal:

$$G^{<}_{\alpha\beta}(\boldsymbol{k},\boldsymbol{k}')=G^{<}_{\alpha\beta}(\boldsymbol{k})\delta(\boldsymbol{k}-\boldsymbol{k}')(2\pi)^3.$$

In reality, equation (8) for the Hamiltonian (1) in the length gauge should be further transformed [20], to explicitly give zero off-diagonal elements, and this could generate additional terms. In our problem these transforms would be complex, so we make the *ansatz* that equation (8) gives momentum-diagonal $G^{<}_{\alpha\beta}$.

The steady-state shift-current density $\boldsymbol{J}$ can be expressed as follows:

$$\boldsymbol{J}=2e\int\frac{\mathrm{d}\hbar\omega}{2\pi}\int\frac{\mathrm{d}\boldsymbol{k}}{(2\pi)^3}\sum_{\alpha\neq\beta}\boldsymbol{v}_{\beta\alpha}(\boldsymbol{k})G^{<}_{\alpha\beta}(\boldsymbol{k},\omega)=\boldsymbol{J}_e+\boldsymbol{J}_s+\boldsymbol{J}_r \tag{12}$$

where the prefactor 2 accounts for the spins. The components $\boldsymbol{J}_{e,s,r}$, which represent the contributions of the three processes depicted in figure 1(a), can be obtained, if $\boldsymbol{v}_{\beta\alpha}$ from (4) and the solution $G^{<}_{\alpha\beta}$ of equation (8) are substituted in expression (12). In the steady state, the first term on the l.h.s. of equation (8) is absent. The remaining $G^{<}_{\alpha\beta}$, expressed through the scattering integrals on the r.h.s., can be substituted in (12), which was also used in reference [21]. In transient situations, the time derivative of $G^{<}_{\alpha\beta}$ in equation (8) must also be included, but we are postponing this problem to future studies. Terms with equal band indices $\alpha=\beta$ in (12) would give the ballistic current density, calculated in reference [4] for excitation by two laser beams.

3.4. The excitation current density $\boldsymbol{J}_e$

Let us first find the expression for $\boldsymbol{J}_e$ from the two terms with $\Sigma_{f;\alpha\beta}$ on the r.h.s. of equation (8). Since $\boldsymbol{J}_e$ results in the second order of the laser field, $\Sigma_{f;\alpha\beta}$ in those terms must be combined with the first-order interband correlation functions $G^{<}_{1;\alpha\beta}\approx(G_{0;\alpha\alpha}\Sigma_{f;\alpha\beta}G_{0;\beta\beta})^{<}$, expressed

through the interacting Green functions in the absence of a laser field [4] $G_{0;\alpha\alpha}$. The resulting $\boldsymbol{J}_e$ has the form

$$\boldsymbol{J}_e = 2\mathrm{i}e \int \frac{\mathrm{d}\omega}{2\pi} \int \frac{\mathrm{d}\boldsymbol{k}}{(2\pi)^3} \sum_{\alpha\neq\beta;\gamma} \boldsymbol{r}_{\beta\alpha}(\boldsymbol{k}) \times \Big(\Sigma^{\pm}_{f;\alpha\gamma}(\boldsymbol{k}, \bar{\boldsymbol{k}}_1) \big(G_{0;\gamma\gamma}(\bar{\boldsymbol{k}}_1, \bar{\boldsymbol{k}}_2, \omega) \Sigma^{\mp}_{f;\gamma\beta}(\bar{\boldsymbol{k}}_2, \bar{\boldsymbol{k}}_3) G_{0;\beta\beta}(\bar{\boldsymbol{k}}_3, \boldsymbol{k}, \omega \pm \omega_0) \big)^{<} - \big(G_{0;\alpha\alpha}(\boldsymbol{k}, \bar{\boldsymbol{k}}_1, \omega) \Sigma^{\mp}_{f;\alpha\gamma}(\bar{\boldsymbol{k}}_1, \bar{\boldsymbol{k}}_2) G_{0;\gamma\gamma}(\bar{\boldsymbol{k}}_2, \bar{\boldsymbol{k}}_3, \omega \pm \omega_0) \big)^{<} \Sigma^{\pm}_{f;\gamma\beta}(\bar{\boldsymbol{k}}_3, \boldsymbol{k}) \Big) \tag{13}$$

where we neglect vertex corrections to $G^{<}_{1;\alpha\beta}$, which can contribute especially in transient situations [4], and assume that $G_{0;\alpha\beta} \approx 0$. We also write two momenta in the equilibrium Green functions $G_{0;\alpha\alpha}(\boldsymbol{k}, \boldsymbol{k}')$, in order to take the derivatives from the field self-energies $\Sigma_{f;\alpha\beta}(\boldsymbol{k}, \boldsymbol{k}')$, even though they fulfil $G_{0;\alpha\alpha}(\boldsymbol{k}, \boldsymbol{k}') = G_{0;\alpha\alpha}(\boldsymbol{k})\delta(\boldsymbol{k} - \boldsymbol{k}')(2\pi)^3$ without the above *ansatz*. In appendix A, we show [16] that after algebraic manipulations only elements with $\gamma = \beta$ ($\gamma = \alpha$) remain in the first (second) expression of equation (13).

Finally, we obtain the c-component of the vector for the current density $\boldsymbol{J}_e$:

$$J^c_e = 2e^3 \int \frac{\mathrm{d}\omega}{2\pi} \int \frac{\mathrm{d}\boldsymbol{k}}{(2\pi)^3} \sum_{\alpha\neq\beta} r^a_{\beta\alpha;c}(\boldsymbol{k}) r^b_{\alpha\beta}(\boldsymbol{k}) E^a_{\pm\omega_0} E^b_{\mp\omega_0} \big(G_{0;\alpha\alpha}(\boldsymbol{k}, \omega) G_{0;\beta\beta}(\boldsymbol{k}, \omega \pm \omega_0) \big)^{<} \tag{14}$$

where the summation over a- and b-components is performed. The sign convention and the terms $r^a_{\beta\alpha;c}(\boldsymbol{k})$ are described in appendix A. For weak scattering, expression (14) agrees with density matrix calculations [16]. In this formalism, also a non-zero virtual term *below* the band gap can be traced in an expression analogous to (14). It can be cancelled by a similar term, with opposite sign, resulting from the band-diagonal contribution $\boldsymbol{v}_{\alpha\alpha} G^{<}_{\alpha\alpha}$ to the current.

For light linearly polarized in the b-direction, the product of the components $E^b_{\pm\omega_0}$ with $r^b_{\beta\alpha;c}(\boldsymbol{k}) r^b_{\alpha\beta}(\boldsymbol{k})$ can be further simplified. If the matrix elements are used in the form [9, 10] $r^b_{\beta\alpha}(\boldsymbol{k}) = |r^b_{\beta\alpha}(\boldsymbol{k})| \mathrm{e}^{\mathrm{i}\phi^b_{\beta\alpha}(\boldsymbol{k})}$, we can arrange $\boldsymbol{J}_e$ as follows:

$$\boldsymbol{J}_e = 2e^3 \int \frac{\mathrm{d}\omega}{2\pi} \int \frac{\mathrm{d}\boldsymbol{k}}{(2\pi)^3} \sum_{\alpha\neq\beta} |E^b_{+\omega_0}|^2 \left(\mathrm{i}\boldsymbol{R}^b_{e;\beta\alpha}(\boldsymbol{k}) |r^b_{\alpha\beta}(\boldsymbol{k})|^2 + \frac{1}{2} \frac{\partial |r^b_{\alpha\beta}(\boldsymbol{k})|^2}{\partial \boldsymbol{k}} \right) \times \big(G_{0;\alpha\alpha}(\boldsymbol{k}, \omega) G_{0;\beta\beta}(\boldsymbol{k}, \omega \pm \omega_0) \big)^{<} \tag{15}$$

where we have introduced the excitation shift vector $\boldsymbol{R}^b_{e;\beta\alpha}$ with the c-component

$$R^{b;c}_{e;\beta\alpha}(\boldsymbol{k}) = \frac{\partial \phi^b_{\beta\alpha}(\boldsymbol{k})}{\partial k^c} + \xi^c_{\alpha\alpha}(\boldsymbol{k}) - \xi^c_{\beta\beta}(\boldsymbol{k}). \tag{16}$$

From expression (16), it follows that the vector is invariant under the phase transformation [9, 10, 16] $\psi_{\beta\boldsymbol{k}}(\boldsymbol{x}) \to \mathrm{e}^{\mathrm{i}\theta_n(\boldsymbol{k})} \psi_{\beta\boldsymbol{k}}(\boldsymbol{x})$ of the Bloch functions $\psi_{\beta\boldsymbol{k}}(\boldsymbol{x})$, where $\theta_n(\boldsymbol{k})$ are arbitrary well-behaved functions. It is also anti-symmetric, $\boldsymbol{R}^b_{e;\beta\alpha}(\boldsymbol{k}) = -\boldsymbol{R}^b_{e;\alpha\beta}(\boldsymbol{k})$, in the band index substitution $\alpha \leftrightarrow \beta$, since $\boldsymbol{r}_{\alpha\beta}(\boldsymbol{k}) = (\boldsymbol{r}_{\beta\alpha}(\boldsymbol{k}))^*$. Note that in (15) the anti-symmetric $\boldsymbol{R}^b_{e;\alpha\beta}(\boldsymbol{k})$ combines with the imaginary (spectral) values from the Green function product, while the band-symmetric derivative $\partial |r^b_{\alpha\beta}(\boldsymbol{k})|^2 / \partial \boldsymbol{k}$ combines with its real (main) part, representing renormalization effects due to interactions. An analogous situation occurs for the scattering shift vector $\boldsymbol{R}_{s;\beta\beta}(\boldsymbol{k}, \boldsymbol{k}')$ (see appendix B) and for the scattering current density $\boldsymbol{J}_s$, discussed below.

3.5. The scattering current density $\boldsymbol{J}_s$

The formula for $\boldsymbol{J}_s$ can be obtained, if the remaining two terms from the r.h.s. of equation (8), with the electron–phonon self-energy in (11), are substituted in expression (12). In this work, we consider only *intraband* relaxation, so band-diagonal Green functions are used in $\boldsymbol{J}_s$. We also assume that they depend on one $\boldsymbol{k}$-variable, in accordance with our *ansatz*.

Let us concentrate first on the two terms $\boldsymbol{r}(\Sigma^R G^< - G^R \Sigma^<)$ in the expression resulting from (12). They can be written as follows:

$$\begin{aligned}
&\sum_{\alpha\neq\beta} \boldsymbol{r}_{\beta\alpha}(\boldsymbol{k})\big(\Sigma^R_{\alpha\beta}(\boldsymbol{k},\omega)G^<_{\beta\beta}(\boldsymbol{k},\omega) - G^R_{\alpha\alpha}(\boldsymbol{k},\omega)\Sigma^<_{\alpha\beta}(\boldsymbol{k},\omega)\big) \\
&\quad = \sum_{\alpha\neq\beta;\gamma} \boldsymbol{r}_{\beta\alpha}(\boldsymbol{k}) M_{\alpha\gamma}(\boldsymbol{k},\boldsymbol{k}-\bar{\boldsymbol{q}}) G^R_{\gamma\gamma}(\boldsymbol{k}-\bar{\boldsymbol{q}},\omega-\bar{\omega}) D^>(\bar{\boldsymbol{q}},\omega-\bar{\omega}) \\
&\qquad \times M_{\gamma\beta}(\boldsymbol{k}-\bar{\boldsymbol{q}},\boldsymbol{k}) G^<_{\beta\beta}(\boldsymbol{k},\omega) \\
&\qquad - \sum_{\alpha\neq\beta;\gamma} \boldsymbol{r}_{\beta\alpha}(\boldsymbol{k}) M_{\alpha\gamma}(\boldsymbol{k},\boldsymbol{k}-\bar{\boldsymbol{q}}) G^<_{\gamma\gamma}(\boldsymbol{k}-\bar{\boldsymbol{q}},\omega-\bar{\omega}) D^R(\bar{\boldsymbol{q}},\omega-\bar{\omega}) \\
&\qquad \times M_{\gamma\beta}(\boldsymbol{k}-\bar{\boldsymbol{q}},\boldsymbol{k}) G^<_{\beta\beta}(\boldsymbol{k},\omega) \\
&\qquad - \sum_{\gamma\neq\alpha;\beta} \boldsymbol{r}_{\alpha\gamma}(\boldsymbol{k}) G^R_{\gamma\gamma}(\boldsymbol{k},\omega) M_{\gamma\beta}(\boldsymbol{k},\boldsymbol{k}-\bar{\boldsymbol{q}}) G^<_{\beta\beta}(\boldsymbol{k}-\bar{\boldsymbol{q}},\omega-\bar{\omega}) D^<(\bar{\boldsymbol{q}},\omega-\bar{\omega}) \\
&\qquad \times M_{\beta\alpha}(\boldsymbol{k}-\bar{\boldsymbol{q}},\boldsymbol{k})
\end{aligned} \tag{17}$$

where the band arguments have been shifted in the last term. In the propagator part of the electron–phonon self-energy, the formula $\Sigma^R \propto (GD)^R = G^R D^> - G^< D^R$ has been used, which is valid for functions with this argument ordering [24, 25]. The first term on the r.h.s. of equation (17), resulting from $G^R D^<$, looks similar to the last term, but the two differ in the type of phonon correlation function $D^>$, $D^<$ and the energy–momentum arguments in $G^<_{\beta\beta}$, $G^R_{\gamma\gamma}$ and $M_{\gamma\beta}$.

This can be changed, if the substitutions $\boldsymbol{k}' = \boldsymbol{k} - \bar{\boldsymbol{q}}$ and $\omega' = \omega - \bar{\omega}$, followed by $\omega'' = -\bar{\omega}$, are used in the last term of (17); we take advantage of the fact that the Bose–Einstein distribution satisfies

$$n_{BE}(\omega) = 1/(\exp(\hbar\omega/kT) - 1) = -(1 + n_{BE}(-\omega)).$$

The sum of the first and last terms is

$$\begin{aligned}
&\Big(\sum_{\alpha\neq\beta;\gamma} \boldsymbol{r}_{\beta\alpha}(\boldsymbol{k}) M_{\alpha\gamma}(\boldsymbol{k},\boldsymbol{k}-\bar{\boldsymbol{q}}) - \sum_{\gamma\neq\alpha;\beta} M_{\beta\alpha}(\boldsymbol{k},\boldsymbol{k}-\bar{\boldsymbol{q}}) \boldsymbol{r}_{\alpha\gamma}(\boldsymbol{k}-\bar{\boldsymbol{q}})\Big) M_{\gamma\beta}(\boldsymbol{k}-\bar{\boldsymbol{q}},\boldsymbol{k}) \\
&\qquad \times G^R_{\gamma\gamma}(\boldsymbol{k}-\bar{\boldsymbol{q}},\omega-\bar{\omega}) D^>(\bar{\boldsymbol{q}},\omega-\bar{\omega}) G^<_{\beta\beta}(\boldsymbol{k},\omega).
\end{aligned} \tag{18}$$

Here the band indices of the electron propagator and correlation function can be set equal, $\gamma = \beta$, because intraband relaxation is considered. The commutator in the large bracket, multiplied by the element $M_{\gamma\beta}(\boldsymbol{k}-\bar{\boldsymbol{q}},\boldsymbol{k})$, can be rewritten in terms of the scattering shift vector $\boldsymbol{R}_{s;\beta\beta}(\boldsymbol{k},\boldsymbol{k}-\bar{\boldsymbol{q}})$ and a renormalization correction, as shown in equation (B.3). If *interband* relaxation is also considered, the resulting formulae can be generalized analogously.

The other two terms $\boldsymbol{r}(\Sigma^< G^A - G^< \Sigma^A)$ in (12) can be reordered similarly, if again just the term $G^A D^<$ in $\Sigma^A \propto (GD)^A = G^A D^> - G^< D^A$ is considered. The remaining terms $-G^< D^R$, $-G^< D^A$ from $(GD)^R$, $(GD)^A$, respectively, can also be summed to this form. Here, the imaginary part of the phonon propagator appears, instead of the electron propagator. Its real part would give further renormalization contributions, if phonon scattering was considered.

We finally have that the scattering shift-current density $\boldsymbol{J}_s$ in the steady state is equal to

$$\begin{aligned}\boldsymbol{J}_s = -4e \int \frac{\mathrm{d}\omega}{2\pi} \int \frac{\mathrm{d}\boldsymbol{k}}{(2\pi)^3} \sum_{\beta} \Bigg\{ \Bigg(& \boldsymbol{R}_{s;\beta\beta}(\boldsymbol{k}, \boldsymbol{k}-\bar{\boldsymbol{q}}) |M_{\beta\beta}(\boldsymbol{k}, \boldsymbol{k}-\bar{\boldsymbol{q}})|^2 \operatorname{Im} G^R_{\beta\beta}(\boldsymbol{k}-\bar{\boldsymbol{q}}, \omega-\bar{\omega}) \\ & - \frac{1}{2} \left(\frac{\partial |M_{\beta\beta}(\boldsymbol{k}-\bar{\boldsymbol{q}}, \boldsymbol{k})|^2}{\partial \boldsymbol{k}} + \frac{\partial |M_{\beta\beta}(\boldsymbol{k}-\bar{\boldsymbol{q}}, \boldsymbol{k})|^2}{\partial (\boldsymbol{k}-\bar{\boldsymbol{q}})} \right) \operatorname{Re} G^R_{\beta\beta}(\boldsymbol{k}-\bar{\boldsymbol{q}}, \omega-\bar{\omega}) \Bigg) \\ & \times D^{>}(\bar{\boldsymbol{q}}, \omega-\bar{\omega}) G^{<}_{\beta\beta}(\boldsymbol{k}, \omega) + \boldsymbol{R}_{s;\beta\beta}(\boldsymbol{k}, \boldsymbol{k}-\bar{\boldsymbol{q}}) |M_{\beta\beta}(\boldsymbol{k}, \boldsymbol{k}-\bar{\boldsymbol{q}})|^2 \\ & \times \frac{1}{4} \big(G^{<}_{\beta\beta}(\boldsymbol{k}-\bar{\boldsymbol{q}}, \omega-\bar{\omega}) - G^{<}_{\beta\beta}(\boldsymbol{k}-\bar{\boldsymbol{q}}, \omega+\bar{\omega}) \big) G^{<}_{\beta\beta}(\boldsymbol{k}, \omega) \Bigg\}. \end{aligned} \tag{19}$$

The intraband correlation functions $G^{<}_{\beta\beta}$ can be obtained from the solution of the KBE similarly to in reference [4]. If the hot-electron population is small, then it is possible to keep in (19) just the terms linear in $G^{<}_{\beta\beta}$.

The renormalization terms in (19), with derivatives of matrix elements, give non-classical corrections to the shift current, due to *quasiparticle* broadening of the carrier spectra. Note, however, that $\boldsymbol{J}_s$ is practically independent of the scattering rate, at least for weak scattering, since $\boldsymbol{R}_{s;\beta\beta}$ is determined by the crystal structure (see appendix B), and the relaxation carrier flow is equal to the injected flow. From the same reason, the temperature dependence of $\boldsymbol{J}_s$ is also weak. Expressions analogous to equations (14), (19) can be derived for the recombination current density $\boldsymbol{J}_r$, but in section 5 we argue that $\boldsymbol{J}_r$ is usually negligible.

4. Approximate solution for the shift currents

Here we approximate the expressions for $\boldsymbol{J}_e$ and $\boldsymbol{J}_s$ to the Boltzmann limit, which can give reasonable results for materials with a moderate scattering. First we simplify $\boldsymbol{J}_e$ in (14), where the light orientation is chosen along the (1, 1, 0) direction, appropriate for GaAs. Next, we approximate the equations for the correlation functions $G^{<}_{\beta\beta}$, and insert their solution in equation (19) for $\boldsymbol{J}_s$, together with the shift vector $\boldsymbol{R}_{s;\beta\beta}$ in (B.3).

4.1. The excitation current density $\boldsymbol{J}_e$

In numerical studies, it is convenient to evaluate $\boldsymbol{J}_e$ from expression (14) even for linearly polarized light, so that *ab initio* calculations of the elements $\boldsymbol{r}_{\beta\alpha}(\boldsymbol{k})$ can be performed along the usual crystal axes. Once evaluated, $\boldsymbol{r}_{\beta\alpha}(\boldsymbol{k})$ can be used to obtain the elements $\boldsymbol{r}_{\beta\alpha;c}(\boldsymbol{k})$ from the formulae (3.36) and (3.37) in reference [15]. For weak scattering, renormalization effects contained in the derivatives $\partial |r^b_{\alpha\beta}(\boldsymbol{k})|^2 / \partial \boldsymbol{k}$ from equation (15) can be neglected, which, in equation (14), is equivalent to taking only the imaginary part of $r^a_{\beta\alpha;c}(\boldsymbol{k}) r^b_{\alpha\beta}(\boldsymbol{k})$, anti-symmetric in the band indices. Then, $G^{<}_{vv} G^{A}_{cc}$ ($\alpha = v$, $\beta = c$) there can be combined with $-G^{R}_{cc} G^{<}_{vv}$ ($\alpha = c$, $\beta = v$), which gives $G^{<}_{vv}(-2\mathrm{i} \operatorname{Im} G^{R}_{cc}) = \mathrm{i} A_{vv} A_{cc}$, where $A_{\alpha\alpha}$ are the electron spectral functions [4]. The terms with exchanged band indices are zero, since in equilibrium the conduction band is empty; i.e. $G^{<}_{cc}(\boldsymbol{k}, \omega) = A_{cc}(\boldsymbol{k}, \omega) n_{FD}(\omega) \approx 0$, where $n_{FD}(\omega) = 1/(\exp(\hbar\omega/kT) + 1)$ is the Fermi–Dirac distribution.

The integration over $\boldsymbol{k}$ and ω in the two spectral functions $A_{vv} A_{cc}$ is performed as in reference [4]. A parabolic approximation for the bands is considered in these integrations (not in $\boldsymbol{r}_{\alpha\beta}(\boldsymbol{k})$), with wave vectors tuned to the resonant values $\boldsymbol{k}^n_{res}$, used to describe electrons that relax between the energy levels $E^n_{res} = E^0_{res} + n\hbar\omega_Q$ (laser tuning to E^0_{res}). The notation for the angles is related to the electric field $\boldsymbol{E}_{\omega_0} = (E_{\omega_0}/\sqrt{2})(1, 1, 0)$; the angle $\phi \in (0, \pi)$ is between the direction (1, 1, 0) and the $\boldsymbol{k}^n_{res}$-vectors, and the angle $\theta \in (0, 2\pi)$ is in the

plane orthogonal to the (1, 1, 0) direction. The non-zero z-component of the excitation current density is ($\eta = (k^0_{res}, \phi, \theta)$)

$$J^z_e = -\mathrm{i}\frac{k^0_{res}e^3}{\hbar^3}\mu_{cv}|E_{\omega_0}|^2\int_0^{2\pi}\frac{\mathrm{d}\theta}{2\pi}\int_0^{\pi}\frac{\mathrm{d}\phi}{2\pi}\sin(\phi)\big(r^x_{cv;z}(\eta)r^y_{vc}(\eta)+r^y_{cv;z}(\eta)r^x_{vc}(\eta)\big) \tag{20}$$

where $\mu_{cv} = m_c m_v/(m_c+m_v)$ is the effective electron–hole mass, and the factor in the bracket is purely imaginary. If the light polarization is in the $(1,-1,0)$ direction, the signs of both terms with x-arguments change. Since the integral is the same, the current is opposite, in agreement with figure 1(b).

4.2. The scattering current density $\boldsymbol{J}_s$

In order to approximate $\boldsymbol{J}_s$ in equation (19), we need first the transport equations for the intraband correlation functions $G^<_{\beta\beta}(\boldsymbol{k},\omega)$. Here we describe the hot-electron relaxation using the integral KBE derived in reference [4]. In the weak-scattering limit, they can be approximated by the integral Boltzmann equation (IBE) [4]. For simplicity, we also describe the hot-carrier population only in the conduction band.

Laser light polarized along the (1, 0, 0) direction, as used in reference [4], gives a nearly isotropic hot-electron distribution in the plane orthogonal to this direction, which is sufficiently described by the angle ϕ. In the present work, polarization along the (1, 1, 0) direction gives a population squeezed in the (0, 0, 1) direction by about 25% (see figure 2, later). Moreover, the shift vectors are also very anisotropic (see figure 3(b), later), so both angular variables ϕ, θ must be used. The field self-energy for *interband* transitions along the (1, 1, 0) direction can be obtained from expression (10) in the form

$$\Sigma^+_{f;cv}(\phi,\theta) = -e\big(r^x_{cv}(k^0_{res},\phi,\theta)+r^y_{cv}(k^0_{res},\phi,\theta)\big)E_{\omega_0}/\sqrt{2}. \tag{21}$$

In the scattering self-energy $\Sigma_{s;cc}$, the matrix elements $M_{cc}(\boldsymbol{k},\boldsymbol{k}')$ contain the linearized structure factors $\gamma_{cc}(\boldsymbol{k},\boldsymbol{k}')$ from (B.10). Since *intraband* relaxation is considered, the square of the exponential prefactor from (B.10) gives $\gamma_{cc}(\boldsymbol{k},\boldsymbol{k}') \approx 1$, i.e. $M_{cc}(\boldsymbol{k},\boldsymbol{k}') = M(\boldsymbol{k}-\boldsymbol{k}')$ from (5).

Then using the steps in reference [4], we arrive at the steady-state IBE:

$$\begin{aligned} f_{cc}(n,\phi,\theta) = \frac{2k^n_{res}\tau_o(n)}{\hbar^3}\Bigg\{&|\Sigma^+_{f;cv}(\phi,\theta)|^2\mu_{cv}\delta_{n0} \\ &+\frac{m_c}{2}M_0^2\int_0^{2\pi}\frac{\mathrm{d}\bar\theta}{2\pi}\int_0^{\pi}\frac{\mathrm{d}\bar\phi}{2\pi}\sin(\bar\phi)\Bigg(\frac{1}{|\boldsymbol{k}^n_{res}-\bar{\boldsymbol{k}}^{n-1}_{res}|^2}f_{cc}(n-1,\bar\phi,\bar\theta)n_B(\omega_Q) \\ &+\frac{1}{|\boldsymbol{k}^n_{res}-\bar{\boldsymbol{k}}^{n+1}_{res}|^2}f_{cc}(n+1,\bar\phi,\bar\theta)(1+n_B(\omega_Q))\Bigg)\Bigg\} \end{aligned} \tag{22}$$

where the distribution function on the nth level ($\varepsilon^\pm_n = E^n_{res} \pm n\hbar\omega_Q/2$)

$$f_{cc}(n,\phi,\theta) = \int_{\varepsilon^-_n}^{\varepsilon^+_n}\frac{\mathrm{d}\hbar\omega}{2\pi}\int_0^{\infty}\frac{\mathrm{d}k}{2\pi}\,k^2G^<_{2;cc}(k,\phi,\theta,\omega) \tag{23}$$

is defined from the second-order $G^< \approx G^<_2/2!$, expanded in terms of the interband field self-energy $\Sigma_{f;cv}$; the prefactor 2 in equation (22) cancels this 2!. Here

$$\tau_0(n) = -\hbar/(2\,\mathrm{Im}\,\Sigma^r_{cc,s}(n))$$

is the particle relaxation time. It is still necessary to add in equation (22) radiative transfers of carriers between the bands, but this is practically not reflected in $\boldsymbol{J}_e$, and $\boldsymbol{J}_r$ is also negligible.

To calculate $\boldsymbol{J}_s$, we also need a simpler expression for the scattering shift vector $\boldsymbol{R}_{s;\beta\beta}(\boldsymbol{k},\boldsymbol{k}')$ in (B.4). A tractable approximation [9, 10] can be obtained if this is linearized in terms of the wave-vector difference $\boldsymbol{k}-\boldsymbol{k}'$, around the centre $\boldsymbol{k}_0=(\boldsymbol{k}'+\boldsymbol{k})/2$. For large differences, where the errors can grow, the contributions to scattering are small, since the elements $|M(\boldsymbol{k}-\boldsymbol{k}')|^2$ decay as $|\boldsymbol{k}-\boldsymbol{k}'|^{-2}$. Direct algebraic manipulation gives the scattering shift vector in (B.11) and (B.12). In the current formula (19), we expand the vector $\boldsymbol{R}_{s;\beta\beta}$ in each wave vector $\boldsymbol{k}$ *considered* in the Brillouin zone.

Finally, expression (19) for $\boldsymbol{J}_s$ can be rewritten in the Boltzmann limit, where

$$A_{\beta\beta}(\boldsymbol{k},\omega)=-2\,\mathrm{Im}\,G^R_{\beta\beta}(\boldsymbol{k},\omega)\approx 2\pi\delta(\hbar\omega-\epsilon_\beta(\boldsymbol{k})).$$

Since the correlation function $D^>(\boldsymbol{q},\omega)$ for free phonons is also sharp, it can easily be convoluted over frequency and momentum with $A_{\beta\beta}(\boldsymbol{k},\omega)$. If we consider in (19) only the term linear in $G^<_{\beta\beta}$, and neglect renormalization factors, then the approximate $\boldsymbol{J}_{s;cc}$ results:

$$\begin{aligned}\boldsymbol{J}_{s;cc}=-\frac{em_cM_0^2}{\hbar^2}\sum_n\int_0^{2\pi}\frac{\mathrm{d}\theta}{2\pi}\int_0^{\pi}\frac{\mathrm{d}\phi}{2\pi}\sin(\phi)f_{cc}(n,\phi,\theta)\int_0^{2\pi}\frac{\mathrm{d}\bar\theta}{2\pi}\int_0^{\pi}\frac{\mathrm{d}\bar\phi}{2\pi}\sin(\bar\phi)\\ \times\left(\frac{k^{n-1}_{res}}{|\boldsymbol{k}^n_{res}-\bar{\boldsymbol{k}}^{n-1}_{res}|^2}(\boldsymbol{k}^n_{res}-\bar{\boldsymbol{k}}^{n-1}_{res})\times\boldsymbol{\Omega}_c(\boldsymbol{k}^n_{res})(1+n_B(\omega_Q))\right.\\ \left.+\frac{k^{n+1}_{res}}{|\boldsymbol{k}^n_{res}-\bar{\boldsymbol{k}}^{n+1}_{res}|^2}(\boldsymbol{k}^n_{res}-\bar{\boldsymbol{k}}^{n+1}_{res})\times\boldsymbol{\Omega}_c(\boldsymbol{k}^n_{res})n_B(\omega_Q)\right).\end{aligned}\tag{24}$$

Here the distribution from (23) has been used, where the integration over ω and $k=|\boldsymbol{k}|$ from equation (19) is already performed. A more consistent approximation in equation (24) can be obtained by evaluating the vectors $\boldsymbol{\Omega}_c$ at the points $(\boldsymbol{k}^n_{res}+\bar{\boldsymbol{k}}^{\pm1}_{res})/2$. Numerically, it is easier to average $\boldsymbol{\Omega}_c$, evaluated at the side points $\boldsymbol{k}^n_{res}$, $\bar{\boldsymbol{k}}^{\pm1}_{res}$.

5. Numerical results and discussion

In applications, we consider a typical experimental configuration for GaAs; the laser intensity is $I=10^6$ W cm^{-2} at the light energy $\hbar\omega_0=2.1$ eV (band gap $E_g=1.5$ eV), with light polarized along the (1, 1, 0) direction. We calculate the steady-state $\boldsymbol{J}_e$ from equation (20), and $\boldsymbol{J}_s$ is obtained by solving equation (22) for the intraband distribution $f_{\beta\beta}(n,\phi,\theta)$, which is then used in equation (24). The recombination current density $\boldsymbol{J}_r$ is also discussed.

We consider a model of GaAs with ten bands, without spin–orbit coupling. The matrix elements $\boldsymbol{r}_{ij}$ are calculated *ab initio* within the density functional theory in the local density approximation using a plane-wave pseudopotential approach [26]. They are obtained at the resonant momentum k^0_{res} (resonant value for the light energy $\hbar\omega_0$) and at about 40 energy (momentum) levels in the band c, corresponding to resonant values of LO phonon processes (E^n_{res} at momenta k^n_{res}). The elements are found on a mesh (ϕ_i,θ_j), which can be reduced due to symmetry to a size 10×20 points in the region $\phi=(0,\pi/2)$, $\theta=(0,\pi)$, giving in total around 100 Mbyte of input data. The calculated current density $\boldsymbol{J}_e$ corresponds to the excitation between the heavy-hole bands ($v=3,4$ in equation (21)) and the lowest conduction band ($c=5$), while $\boldsymbol{J}_s$ is illustrated only for the band $c=5$.

5.1. The electron distributions

In figure 2, we show cross-sections, orthogonal to the (1, 1, 0) direction, through the electron population $f_{cc}(n,\phi,\theta)$ in the conduction band, multiplied by $\sin(\phi)$ as in equation (24). The solid and four dashed lines on each plot correspond to the angles $\phi=i\pi/10$ ($i=5,\ldots,1$),

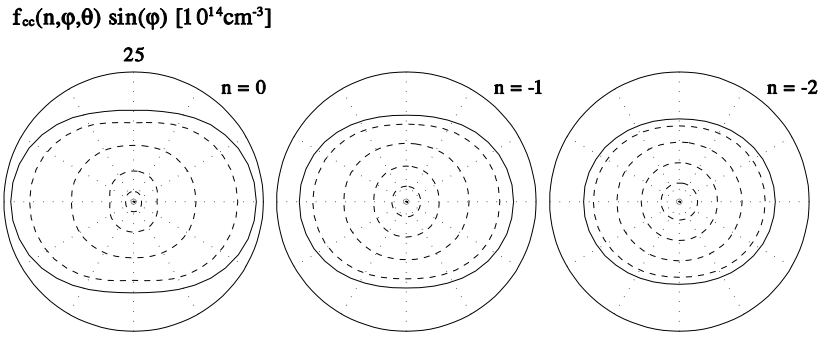

Figure 2. Cross-sections through the population $f_{cc}(n, \phi, \theta)$, multiplied by $\sin(\phi)$, in the planes orthogonal to the (1, 1, 0) direction. The values for levels $n = 0, -1, -2$ show relaxation of the squeezing along the (0, 0, 1) and (1, 1, 0) directions. The solid and four dashed lines correspond to the angles $\phi = i\pi/10$ ($i = 5, \ldots, 1$).

while the shapes of the ovals give the θ-distribution. The levels presented are $n = 0, -1, -2$, and the temperature is $T = 300$ K. Note that the population ($n = 0$) is squeezed in the (0, 0, 1) and (1, 1, 0) directions, where the latter is seen in the fast decays with ϕ of the ovals for $n = 0$. The population squeezed in the plane orthogonal to the (1, 1, 0) direction, around $\phi \approx 0$, contributes more to the shift current than the population in the plane orthogonal to the (1, −1, 0) direction. Therefore, these contributions with opposite signs do not cancel, and J_e^z can be non-zero. For light polarized in the (1, −1, 0) direction, the population is squeezed in the orthogonal direction, according to the change in $|r_{cv}^x \pm r_{cv}^y|^2$ from (21), and J_e^z changes sign. At lower levels both squeezings become relaxed, which visibly shrinks the size of the population. Relaxation of the anisotropy in hot-carrier distributions was also studied in reference [27].

5.2. The shift-current density $\boldsymbol{J}_e$

In figure 3(a), we show the angular dependence of $\Delta_{rr} = \mathrm{Im}(r_{cv;z}^x r_{vc}^y + r_{cv;z}^y r_{vc}^x)$, multiplied by $\sin(\phi)$, from expression (20) for $\boldsymbol{J}_e$. It is calculated for the angles as in figure 2, and for the light polarized in the (1, 1, 0) direction. If the light is polarized in the (1, −1, 0) direction, Δ_{rr} looks the same, but the prefactor in equation (20) changes sign. This reflects the fact that the structure of GaAs allows pumping from different atoms in both situations, but it gives $\boldsymbol{J}_e = 0$ for excitation by unpolarized light. For the present excitation, we obtain from equation (20) the value $J_e^z \approx -45$ A cm^{-2}. This agrees in sign with figure 1(b) (negative charge of electrons) and in value with reference [16].

5.3. The scattering current density $\boldsymbol{J}_s$

Evaluation of $\boldsymbol{J}_s$ is sensitive to numerical errors, resulting from approximate integrations on the finite mesh for ϕ, θ. We have corrected three problems in the calculation of $\boldsymbol{J}_{s;cc}$. First, it is the flow between level n and $n \pm 1$; second, the conservation of homogeneous distributions (used as an initial test) in scattering between level n and $n \pm 1$; and third, the fact that non-zero shift currents might result even for homogeneous distributions, which is a non-physical consequence of the rough mesh and other approximations.

In figure 3(b), we show the z-component of the linearized scattering shift vector $R_{s;cc}^z$ from the level $n = 0$; the cross-section is orthogonal to the (1, 1, 0) direction at $\phi = \pi/2$.

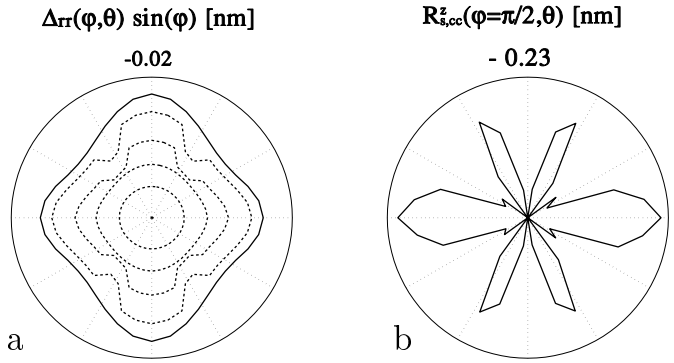

Figure 3. Panel (a) shows the angular dependence of the factor $\Delta_{rr} = \mathrm{Im}(r^x_{cv;z} r^y_{vc} + r^y_{cv;z} r^x_{vc})$, multiplied by $\sin(\phi)$, calculated from the level $n = 0$. The cross-sections are in the plane orthogonal to the polarization direction of light $(1, 1, 0)$. It is opposite if light is polarized in the direction $(1, -1, 0)$. This proves the mechanism in figure 1(b) to be correct, with zero current J^z_e for excitation by unpolarized light. In panel (b) we present the approximate scattering shift vector $\boldsymbol{R}^z_{s;cc}(\phi = \pi/2, \theta) \approx (-\boldsymbol{k} \times \boldsymbol{\Omega}_c)^z$, calculated from the level $n = 0$. The cross-section is as in (a). For the orthogonal cross-section, the contributions only change sign. Thus $J^z_{s;cc} = 0$ for homogeneous electron distribution, resulting approximately for excitation by unpolarized light.

The behaviour of $R^z_{s;cc}$ can be appreciated, if we substitute for the difference of wave vectors in (B.11) and (B.12) with $-\boldsymbol{k}$. This is because, on average, the wave vector $\boldsymbol{k}$ of the excited electron becomes scattered in the $-\boldsymbol{k}$-direction, even though the size k^0_{res} of $-\boldsymbol{k}$ is about an order of magnitude larger than the difference $k^0_{res} - k^{\pm 1}_{res}$. The vector $R^z_{s;cc}$ changes sign, if the cross-section is orthogonal to the $(1, -1, 0)$ direction, providing zero current for a homogeneous distribution. Because of the symmetry specified above, we can limit calculations to one quarter of the Brillouin zone. Note that $R^z_{s;cc}$ has greater magnitude in the horizontal direction, where the squeezed population in figure 2 is also larger, so $J^z_{s;cc}$ becomes increased.

In figure 4(a), we present contributions to $J^z_{s;cc}$ from different electron levels in the conduction band, as induced by phonon scattering [4]. The temperature is $T = 300$ K, and the dashed, solid and dash–dotted lines correspond to the light excitation at the energies corresponding to the levels $n = -2, 0, 2$ (using the same injection rate). The three results are very different, since the shift vector $R^z_{s;cc}$ and, consequently, $J^z_{s;cc}$ change sign around level $n = 0$ (see also figure 5). This effect is related to the form of the matrix elements, and it appears by chance close to the level $n = 0$.

The contributions to the current density $J^z_{s;cc}$ are summed and presented in figure 4(b) in the range $T = 50$–300 K. The excitation energies are labelled by the level number $n = 0, 5, 10$. In this interval the response changes sign, as expected from figure 4(a). $J^z_{s;cc}$ is about three orders of magnitude smaller than J^z_e, but it increases for larger excitation energies (see figure 5). For excitation around $n = 0$, $J^z_{s;cc}$ is nearly temperature independent, while away from $n = 0$ it grows in size with T. In general the increase is small, since $J^z_{s;cc}$ depends weakly on the scattering strength (see the discussion of equation (19)).

In figure 5, we show the dependence of the ratio $J^z_{s;cc}/J^z_e$ on the excitation energy, labelled as in figure 4(b). As already mentioned, the ratio is negative close to the Γ point; it changes sign around $n = 0$ and approaches 1% at $n = 15$. Here we stop our calculations, since the departure from the parabolic band approximation is large. The solid (dashed) curves correspond to $T = 300$ K ($T = 50$ K). Since J^z_e roughly increases by 25% in this energy region, $J^z_{s;cc}$ is responsible for the increased value of the ratio. Note also that at higher excitation

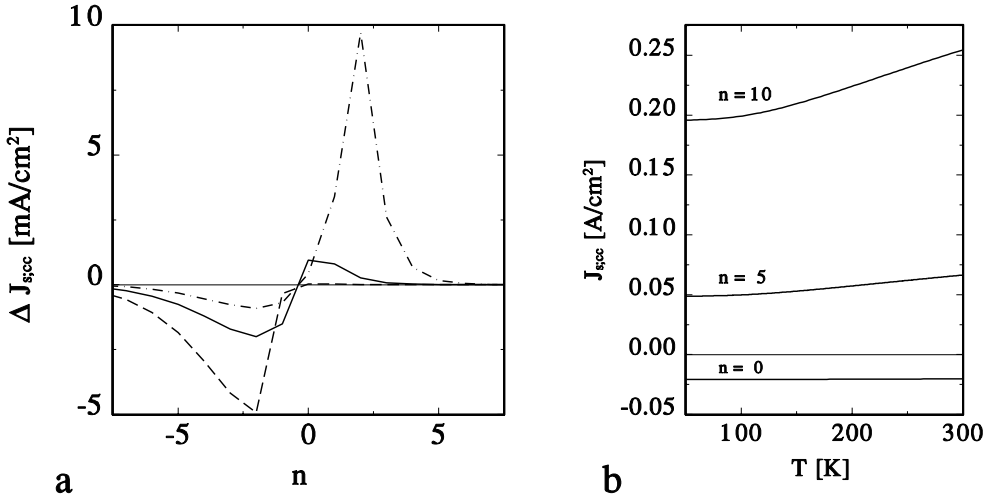

Figure 4. Panel (a) shows contributions to the scattering shift-current density $J^z_{s;cc}$ from different 'electron levels', due to scattering on LO phonons at $T = 300$ K. The dashed, solid and dot–dashed lines correspond to tuning the laser to the energy of the level $n = -2, 0, 2$. The change of sign of the contributions is due to the fact that $R^z_{s;cc}$ at angles $\phi = \pi/2$ changes sign at these excitation energies. In panel (b) we present the temperature dependence of the scattering shift-current density $J^z_{s;cc}$ calculated as a sum of its components in (a). The situations correspond to tuning the laser energy to the levels $n = 0, 5, 10$. $J^z_{s;cc}$ changes sign and slightly increases with temperature, especially at larger n.

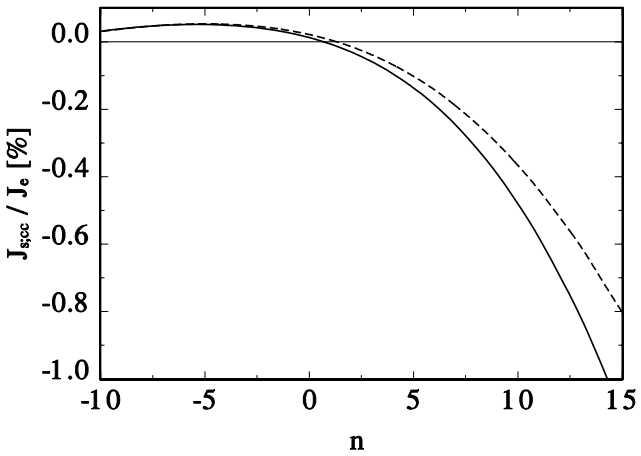

Figure 5. The ratio of the scattering and excitation shift-current densities $J_{s;cc}/J_e$, calculated as a function of excitation energy, labelled in phonon levels. The solid (dashed) lines correspond to $T = 300$ K ($T = 50$ K). The ratio changes sign around $n = 0$ from positive to negative and increases in value up to 1% for the present excitation energies.

energies the current density $J^z_{s;cc}$ is *opposite* to J^z_e, which could be intuitively expected. The ratio can be larger for relaxation to/from local side minima in the band structure.

5.4. The recombination current density $\boldsymbol{J}_r$

Finally, let us briefly discuss the recombination current density $\boldsymbol{J}_r$. Since the momentum relaxation time τ_p is several hundreds of fs, and the recombination time τ_r is about 1 ns, only a tiny fraction of carriers recombine before randomizing their momenta. The hot carriers first isotropically fill the Brillouin zone, and in particular the distribution is practically the same

in the $(1, 1, 0)$ and $(1, -1, 0)$ directions. It is useful to recognize that $\boldsymbol{J}_e$ and $\boldsymbol{J}_r$ resulting from transitions between two particular states have opposite signs. Therefore, contributions to $\boldsymbol{J}_r$ from the population in the above directions are the same in magnitude, but they point in the $(0, 0, -1)$ and $(0, 0, 1)$ directions. This means that $\boldsymbol{J}_r$ is practically zero, as suggested by figure 1(b), where the recombining electrons going from Ga atoms do not distinguish between the As atoms. The same observation is expressed in reference [1] in a more general way—namely, by saying that $\boldsymbol{J}_r$ is zero in non-pyroelectric materials.

Recombination through trap sites from impurities would give non-zero *microscopic* shift currents, but its macroscopic value $\boldsymbol{J}_r$ averaged over all impurity positions should be negligible. It would also be interesting to study the shift current related to transitions to excitonic levels. Since these levels are energetically below the band edge, they can be expected to give different (smaller) shifts in real space than in the interband transitions. These shifts would also vary level by level, and $\boldsymbol{J}_r$ could also be non-zero.

6. Conclusions

We have theoretically investigated laser beam generation of the shift-current density in bulk NCS semiconductors. The excitation, scattering and recombination components $\boldsymbol{J}_{e,s,r}$ reflect *asymmetric carrier flows* in elementary cells, induced by the relevant processes. The system was described by NGF methods, which, in combination with the length gauge, give a consistent approach to this problem. Expressions for $\boldsymbol{J}_{e,s}$ were derived for steady-state excitations, in terms of the carrier transition rates and the space shift vectors $\boldsymbol{R}_{e,s}$.

For practical purposes, we have simplified the formalism to the Boltzmann limit and demonstrated a tractable numerical scheme. Within this approximation, we have described optically excited GaAs in the presence of LO phonon scattering. Light-induced electron transitions between the lowest conduction band and the nearest heavy-hole bands were considered. For light polarized in the $(1, 1, 0)$ direction, the excitation current density $\boldsymbol{J}_e$ in the $(0, 0, -1)$ direction was obtained. The scattering current density $\boldsymbol{J}_{s;cc}$ was calculated from the hot-electron distribution in the conduction band. It is about two orders of magnitude smaller than $\boldsymbol{J}_e$, and the recombination current density $\boldsymbol{J}_r$ can be neglected, since the momentum relaxation causes electrons to recombine with the same strength with atoms placed in opposite directions. Therefore, *steady-state pumping* of electrons across the crystal can be realized.

The shift current has potential applications in ultrafast photoelectric devices, since the response is practically instantaneous. Modifications of the shift current might be observed in low-dimensional structures, heteropolar nanotubes [28] or molecular systems.

Acknowledgments

The author would like to thank J E Sipe for many discussions of the problem studied and is grateful for financial support provided by Photonic Research Ontario. He acknowledges B Adolf and A Shkrebtii for evaluation of *ab initio* matrix elements. The work was greatly improved with the help of K Busch and as a result of comments from A P Jauho.

Appendix A

Let us first compare current expressions from reference [16] with our results. The sum of the term $\langle J^a_{intra}\rangle^{\mathrm{I}}$ and $\mathrm{d}\langle \boldsymbol{P}^{(2)}_{inter}\rangle/\mathrm{d}t$, there, corresponds to the excitation shift-current density $\boldsymbol{J}_e$ from our equation (12), if scattering is neglected. The term $\langle J^a_{intra}\rangle^{\mathrm{II}}$ there corresponds to the

excitation part of the ballistic current—equation (12) with equal bands $\alpha = \beta$, and no transport vertex corrections to $G^<_{\alpha\alpha}$.

Next, we show how equation (14) can be obtained from equation (13), in analogy to reference [16]. Two situations can be considered in (13), where either one of the two field self-energies $\Sigma^{\pm}_{f;\alpha\beta}$ involved is interband and the other is intraband, or both of them are interband. In the first case, the *interband* self-energy in equation (13) is between the two Green functions, since these are from different bands (empty/full), to give real transitions. The *intraband* self-energy in front or behind can be switched by partial integration (see the comment near (9)) to give a derivative, with a prefactor 1, over the first or last variable in the first or second term in equation (13) with $G^<_{1;\alpha\beta}$. These two can be combined into a derivative $\partial G^<_{1;\alpha\beta}(\boldsymbol{k},\boldsymbol{k})/\partial\boldsymbol{k}$, and transferred by partial integration to the derivative in the prefactor [16] $-\partial \boldsymbol{r}_{\alpha\beta}(\boldsymbol{k})/\partial\boldsymbol{k}$. The resulting contribution to $\boldsymbol{J}_e$ in (13) is

$$\Delta\boldsymbol{J}_e = 2\mathrm{i}e^3 \int \frac{\mathrm{d}\omega}{2\pi} \int \frac{\mathrm{d}\boldsymbol{k}}{(2\pi)^3} \sum_{\alpha\neq\beta} (-\mathrm{i}\boldsymbol{r}_{\beta\alpha;a}(\boldsymbol{k}) r^b_{\alpha\beta}(\boldsymbol{k})) E^a_{\mp\omega_0} E^b_{\pm\omega_0} \times \big(G_{0;\alpha\alpha}(\boldsymbol{k},\omega) G_{0;\beta\beta}(\boldsymbol{k},\omega\pm\omega_0)\big)^< \tag{A.1}$$

where we employ the definition [16]

$$\boldsymbol{r}_{\beta\alpha;a}(\boldsymbol{k}) = \frac{\partial \boldsymbol{r}_{\beta\alpha}(\boldsymbol{k})}{\partial k^a} - \mathrm{i}(\xi^a_{\beta\beta}(\boldsymbol{k}) - \xi^a_{\alpha\alpha}(\boldsymbol{k}))\boldsymbol{r}_{\beta\alpha}(\boldsymbol{k}). \tag{A.2}$$

In (A.1) the sum over bands $\alpha \neq \beta$ selects real transitions between valence and conduction bands, tuned to the laser frequency ω_0. Then, the top (bottom) signs correspond to $\alpha = c$, $\beta = v$ ($\alpha = v$, $\beta = c$).

The second situation adds the expression $\boldsymbol{r}_{\beta\alpha}(\boldsymbol{k}) \sum_{\gamma\neq\alpha,\beta} \big[\xi^a_{\alpha\gamma}(\boldsymbol{k})\xi^b_{\gamma\beta}(\boldsymbol{k}) - \xi^b_{\alpha\gamma}(\boldsymbol{k})\xi^a_{\gamma\beta}(\boldsymbol{k})\big]$ to the bracket $(-\mathrm{i}\boldsymbol{r}_{\beta\alpha;a}(\boldsymbol{k})\xi^b_{\alpha\beta}(\boldsymbol{k}))$ in (A.1). These terms can be substantially simplified with the following identity [16]:

$$r^a_{\alpha\beta;b}(\boldsymbol{k}) - r^b_{\alpha\beta;a}(\boldsymbol{k}) = \mathrm{i} \sum_{\gamma\neq\alpha,\beta} \big[\xi^b_{\alpha\gamma}(\boldsymbol{k})\xi^a_{\gamma\beta}(\boldsymbol{k}) - \xi^a_{\alpha\gamma}(\boldsymbol{k})\xi^b_{\gamma\beta}(\boldsymbol{k})\big] \tag{A.3}$$

which can be used to exchange the vector (b) and derivative (a) components in $r^b_{\alpha\beta;a}(\boldsymbol{k})$. If we substitute (A.3) in (A.1), and shift arguments, then the square brackets cancel and expression (14) results.

Appendix B

Here we derive the expression for the intraband scattering shift vector $\boldsymbol{R}_{s;\beta\beta}(\boldsymbol{k},\boldsymbol{k}')$, used in equation (19), and linearize it in the wave-vector difference $\boldsymbol{k} - \boldsymbol{k}'$.

We assume [9, 10] that the commutator of the operator $\boldsymbol{x}$ in (2) and $\boldsymbol{M}$ in (5) vanishes, i.e., $[\boldsymbol{x}, \boldsymbol{M}] = 0$. In the Bloch representation, we can easily sum over intermediate states and momenta. Upon separating out the terms of the position operator that are band diagonal, we arrive at the following sum rule:

$$\sum_{\alpha\neq\beta} \boldsymbol{r}_{\beta\alpha}(\boldsymbol{k}) M_{\alpha\gamma}(\boldsymbol{k},\boldsymbol{k}') - \sum_{\alpha\neq\gamma} M_{\beta\alpha}(\boldsymbol{k},\boldsymbol{k}')\boldsymbol{r}_{\alpha\gamma}(\boldsymbol{k}') = -\mathrm{i}\left(\frac{\partial}{\partial\boldsymbol{k}} + \frac{\partial}{\partial\boldsymbol{k}'}\right) M_{\beta\gamma}(\boldsymbol{k},\boldsymbol{k}') + M_{\beta\gamma}(\boldsymbol{k},\boldsymbol{k}')(\xi_{\gamma\gamma}(\boldsymbol{k}') - \xi_{\beta\beta}(\boldsymbol{k})). \tag{B.1}$$

Aided by equation (B.1) and writing the matrix elements $M_{\beta\beta}(\boldsymbol{k},\boldsymbol{k}')$ in the form

$$M_{\beta\beta}(\boldsymbol{k},\boldsymbol{k}') = |M_{\beta\beta}(\boldsymbol{k},\boldsymbol{k}')| \mathrm{e}^{\mathrm{i}\phi_{\beta\beta}(\boldsymbol{k},\boldsymbol{k}')} \tag{B.2}$$

it is now straightforward to simplify the bracketed terms in equation (18) for $\gamma = \beta$:

$$\left(\sum_{\alpha\neq\beta} r^c_{\beta\alpha}(\boldsymbol{k})M_{\alpha\beta}(\boldsymbol{k},\boldsymbol{k}') - \sum_{\beta\neq\alpha} M_{\beta\alpha}(\boldsymbol{k},\boldsymbol{k}')r^c_{\alpha\beta}(\boldsymbol{k}')\right)M_{\beta\beta}(\boldsymbol{k}',\boldsymbol{k})$$
$$= R^c_{s;\beta\beta}(\boldsymbol{k},\boldsymbol{k}')|M_{\beta\beta}(\boldsymbol{k}',\boldsymbol{k})|^2 - \frac{\mathrm{i}}{2}\left(\frac{\partial}{\partial k^c} + \frac{\partial}{\partial k'^c}\right)|M_{\beta\beta}(\boldsymbol{k}',\boldsymbol{k})|^2. \tag{B.3}$$

Here the c-component of the scattering shift vector $\boldsymbol{R}_{s;\beta\beta}(\boldsymbol{k},\boldsymbol{k}')$ is

$$R^c_{s;\beta\beta}(\boldsymbol{k},\boldsymbol{k}') = \left(\frac{\partial}{\partial k^c} + \frac{\partial}{\partial k'^c}\right)\phi_{\beta\beta}(\boldsymbol{k},\boldsymbol{k}') + \xi^c_{\beta\beta}(\boldsymbol{k}') - \xi^c_{\beta\beta}(\boldsymbol{k}). \tag{B.4}$$

It has properties similar to those of the excitation shift vector $\boldsymbol{R}_{e;\alpha\beta}(\boldsymbol{k})$ in (16). $\boldsymbol{R}_{s;\beta\beta}(\boldsymbol{k},\boldsymbol{k}')$ is invariant under phase transformations of Bloch functions, and anti-symmetric upon exchanging $\boldsymbol{k}$ and $\boldsymbol{k}'$, i.e. $\boldsymbol{R}_{s;\beta\beta}(\boldsymbol{k},\boldsymbol{k}') = -\boldsymbol{R}_{s;\beta\beta}(\boldsymbol{k}',\boldsymbol{k})$, which follows directly from equation (B.2). Therefore, the real (first) part in equation (B.3) is also anti-symmetric, while the imaginary (second) part is symmetric, and these two give different contributions to the scattering shift-current density $\boldsymbol{J}_s$.

Numerically, it is more convenient to evaluate the shift vector directly from the matrix elements $M_{\alpha\beta}(\boldsymbol{k},\boldsymbol{k}')$, which are accessible to *ab initio* calculations. Then, considerable care has to be taken in order to maintain the invariance under phase transformations. We make use of the specific form of $M_{\beta\beta}(\boldsymbol{k},\boldsymbol{k}')$, with the structure factors $\gamma_{\beta\beta}(\boldsymbol{k},\boldsymbol{k}')$ given in equation (5), to evaluate $R^c_{s;\beta\beta}(\boldsymbol{k},\boldsymbol{k}')$ from

$$R^c_{s;\beta\beta}(\boldsymbol{k},\boldsymbol{k}') = \mathrm{Im}\left[\frac{1}{|\gamma_{\beta\beta}(\boldsymbol{k},\boldsymbol{k}')|^2}\gamma^*_{\beta\beta}(\boldsymbol{k},\boldsymbol{k}')\left(\frac{\partial}{\partial k^c} + \frac{\partial}{\partial k'^c}\right)\gamma_{\beta\beta}(\boldsymbol{k},\boldsymbol{k}')\right] + \xi^c_{\beta\beta}(\boldsymbol{k}') - \xi^c_{\beta\beta}(\boldsymbol{k}). \tag{B.5}$$

Since $\gamma_{\beta\beta}(\boldsymbol{k},\boldsymbol{k}')$ only depends on the band structure, it is clear that the shift vector $\boldsymbol{R}_{s;\beta\beta}$ is an *intrinsic property of the material* and does not depend on the nature of the scattering mechanism.

Equation (B.5) can be used once the $\gamma_{\beta\beta}(\boldsymbol{k},\boldsymbol{k}')$ are found. For practical evaluations it is much easier to obtain their linearized form in the difference $\boldsymbol{k} - \boldsymbol{k}'$. We can evaluate $u_{\beta\boldsymbol{k}}(\boldsymbol{x})$ and $u_{\beta\boldsymbol{k}'}(\boldsymbol{x})$ as well as their derivatives from $u_{\beta\boldsymbol{k}_0}(\boldsymbol{x})$ at $\boldsymbol{k}_0 = (\boldsymbol{k}+\boldsymbol{k}')/2$ using $\boldsymbol{k}\cdot\boldsymbol{p}$ perturbation theory [29]. This allows us to obtain corresponding perturbation theoretical expressions for $\gamma_{\beta\beta}(\boldsymbol{k},\boldsymbol{k}')$, $\xi_{\beta\beta}(\boldsymbol{k})$ and the shift vector $\boldsymbol{R}_{s;\beta\beta}(\boldsymbol{k},\boldsymbol{k}')$.

The linearized $u_{\beta\boldsymbol{k}}(\boldsymbol{x})$ results in the form

$$u_{\beta\boldsymbol{k}_0+\Delta\boldsymbol{k}}(\boldsymbol{x}) = \mathrm{e}^{-\mathrm{i}\xi_{\beta\beta}(\boldsymbol{k}_0)\,\Delta\boldsymbol{k}}\left(u_{\beta\boldsymbol{k}_0}(\boldsymbol{x}) - \mathrm{i}\,\Delta\boldsymbol{k}\sum_{\alpha\neq\beta}\boldsymbol{r}_{\alpha\beta}(\boldsymbol{k}_0)u_{\alpha\boldsymbol{k}_0}(\boldsymbol{x})\right) \tag{B.6}$$

where $\Delta\boldsymbol{k} = \boldsymbol{k} - \boldsymbol{k}_0$. The exponential prefactor reflects the change of the phase in the Bloch wave $u_{\beta\boldsymbol{k}_0+\Delta\boldsymbol{k}}(\boldsymbol{x})$, which is otherwise completely undetermined. As mentioned above, this phase is of paramount importance, since we have to take derivatives with respect to $\boldsymbol{k}$ from the Bloch wave $u_{\beta\boldsymbol{k}_0+\Delta\boldsymbol{k}}(\boldsymbol{x})$ (see equation (B.5)). Therefore, we have to consider *all* $\boldsymbol{k}$-dependencies of $u_{\beta\boldsymbol{k}_0+\Delta\boldsymbol{k}}(\boldsymbol{x})$ to ensure phase transformation invariance of our results. In addition, it follows directly from equation (B.6) that

$$\frac{\partial u_{\beta\boldsymbol{k}}(\boldsymbol{x})}{\partial\boldsymbol{k}} = -\mathrm{i}\xi_{\beta\beta}u_{\beta\boldsymbol{k}}(\boldsymbol{x}) - \mathrm{i}\sum_{\alpha\neq\beta}\boldsymbol{r}_{\alpha\beta}(\boldsymbol{k})u_{\alpha\boldsymbol{k}}(\boldsymbol{x}) \tag{B.7}$$

which is consistent with equation (3), since the fast components of Bloch functions $u_{\alpha\boldsymbol{k}}(\boldsymbol{x})$ and $u^*_{\beta\boldsymbol{k}}(\boldsymbol{x})$ are orthogonal in the unit cell.

Using in equation (B.5) the derivative of expression (5), taken with the help of equation (B.7), gives the exact results

$$\begin{aligned} R^c_{s;\beta\beta}(\boldsymbol{k},\boldsymbol{k}') &= \frac{1}{|\gamma_{\beta\beta}(\boldsymbol{k},\boldsymbol{k}')|}\,\mathrm{Im}[\mathrm{i}\gamma^*_{\beta\beta}(\boldsymbol{k},\boldsymbol{k}')\boldsymbol{\rho}^c_{s;\beta\beta}(\boldsymbol{k},\boldsymbol{k}')] \\ \boldsymbol{\rho}^c_{s;\beta\beta}(\boldsymbol{k},\boldsymbol{k}') &= \sum_{\alpha\neq\beta}(r^c_{\beta\alpha}(\boldsymbol{k})\gamma_{\alpha\beta}(\boldsymbol{k},\boldsymbol{k}') - \gamma_{\beta\alpha}(\boldsymbol{k},\boldsymbol{k}')r^c_{\alpha\beta}(\boldsymbol{k}')). \end{aligned} \tag{B.8}$$

Equation (B.6) may now be used to obtain the $\boldsymbol{k}\cdot\boldsymbol{p}$ perturbation expression for $\boldsymbol{r}_{\beta\alpha}(\boldsymbol{k})$:

$$\boldsymbol{r}_{\beta\alpha}(\boldsymbol{k}) = \mathrm{e}^{\mathrm{i}(\xi_{\beta\beta}(\boldsymbol{k}_0)-\xi_{\alpha\alpha}(\boldsymbol{k}_0))\,\Delta\boldsymbol{k}}\left(\boldsymbol{r}_{\beta\alpha}(\boldsymbol{k}_0) + \sum_{\gamma\neq\beta}\sum_{\sigma\neq\alpha}(\Delta\boldsymbol{k}\cdot\boldsymbol{r}_{\beta\gamma}(\boldsymbol{k}_0))\boldsymbol{r}_{\sigma\alpha}(\boldsymbol{k}_0)\delta_{\gamma\sigma}\right). \tag{B.9}$$

Similarly, one can obtain the expression for $\gamma_{\beta\alpha}(\boldsymbol{k},\boldsymbol{k}')$:

$$\gamma_{\beta\alpha}(\boldsymbol{k},\boldsymbol{k}') = \mathrm{e}^{\mathrm{i}(\xi_{\beta\beta}(\boldsymbol{k}_0)\,\Delta\boldsymbol{k}-\xi_{\alpha\alpha}(\boldsymbol{k}_0)\,\Delta\boldsymbol{k}')}\left(\delta_{\beta\alpha} - \mathrm{i}\,\Delta\boldsymbol{k}\cdot\sum_{\sigma\neq\alpha}\boldsymbol{r}_{\sigma\alpha}(\boldsymbol{k}_0)\delta_{\beta\sigma} + \mathrm{i}\,\Delta\boldsymbol{k}'\cdot\sum_{\beta\neq\sigma}\boldsymbol{r}_{\beta\sigma}(\boldsymbol{k}_0)\delta_{\sigma\alpha}\right) \tag{B.10}$$

where $\Delta\boldsymbol{k} = \boldsymbol{k} - \boldsymbol{k}_0$, $\Delta\boldsymbol{k}' = \boldsymbol{k}' - \boldsymbol{k}_0$. Upon inserting these results in expression (B.8) and making use of the vector identity $\boldsymbol{a}\times(\boldsymbol{b}\times\boldsymbol{c}) = \boldsymbol{b}(\boldsymbol{a}\cdot\boldsymbol{c}) - \boldsymbol{c}(\boldsymbol{a}\cdot\boldsymbol{b})$, we finally arrive at the linearized expression for the scattering shift vector:

$$\boldsymbol{R}_{s;\beta\beta}(\boldsymbol{k},\boldsymbol{k}') \approx (\boldsymbol{k}-\boldsymbol{k}')\times\boldsymbol{\Omega}_\beta(\boldsymbol{k}_0) \tag{B.11}$$

where the vector $\boldsymbol{\Omega}_\beta(\boldsymbol{k}_0)$ is defined as

$$\boldsymbol{\Omega}_\beta(\boldsymbol{k}_0) = \boldsymbol{\nabla}_k\times\boldsymbol{\xi}_{\beta\beta}(\boldsymbol{k}_0) = \mathrm{i}\sum_{\alpha\neq\beta}\boldsymbol{r}_{\beta\alpha}(\boldsymbol{k}_0)\times\boldsymbol{r}_{\alpha\beta}(\boldsymbol{k}_0). \tag{B.12}$$

The last expression for $\boldsymbol{\nabla}_k\times\boldsymbol{\xi}_{\beta\beta}(\boldsymbol{k}_0)$ is also derived in reference [30] (equation (13)). A standard analysis using the symmetry properties [14, 17] of the $\boldsymbol{r}_{\alpha\beta}(\boldsymbol{k}_0)$ shows that $\boldsymbol{\Omega}_\beta(\boldsymbol{k}_0)$ represents an axial pseudo-vector [10] and, as a consequence, can be non-zero only if the material does not possess a centre of inversion. It can be evaluated numerically from *ab initio* values of the respective matrix elements.

References

[1] Sturman B I and Fridkin V M 1992 *The Photovoltaic and Photorefractive Effects in Non-Centrosymmetric Materials (Ferroelectricity and Related Phenomena vol 8)* ed G W Taylor (London: Gordon and Breach Science) and references therein

[2] Kurizki G, Shapiro M and Brumer P 1989 *Phys. Rev.* B **39** 3435

[3] Dupont E *et al* 1995 *Phys. Rev. Lett.* **74** 3596
Atanasov R *et al* 1996 *Phys. Rev. Lett.* **76** 1703

[4] Král P and Sipe J 2000 *Phys. Rev.* B **61** 5381

[5] Král P and Tománek D 1999 *Phys. Rev. Lett.* **82** 5373
Mele E J, Král P and Tománek D 2000 *Phys. Rev.* B **61** 7669

[6] Luttinger J M 1958 *Phys. Rev.* **112** 739

[7] Kraut W and von Baltz R 1979 *Phys. Rev.* B **19** 1548
Kraut W and von Baltz R 1981 *Phys. Rev.* B **23** 5590

[8] Kristoffel N and Gulbis A 1980 *Z. Phys.* B **39** 143

[9] Belinicher V I, Ivchenko E L and Sturman B I 1983 *Sov. Phys.–JETP* **56** 359

[10] Busch K 1992 *Diploma Thesis* University of Karlsruhe

[11] Belinicher V I and Sturman B I 1988 *Ferroelectrics* **83** 29

[12] Rasulov R Ya *et al* 1999 *Semiconductors* **33** 45 and references therein

[13] Král P and Sipe J E 2000 *Progress in Nonequilibrium Green's Functions* ed M Bonitz (Singapore: World Scientific)

[14] Blount E I 1962 *Solid State Physics, Advances in Research and Applications* vol 13, ed F Seitz and D Turnbull (New York: Academic) p 305
[15] Sipe J E and Ghahramani E 1993 *Phys. Rev.* B **48** 11 705
[16] Sipe J E and Shkrebtii A 2000 *Phys. Rev.* B **61** 5337
[17] Madelung O 1978 *Introduction to Solid State Theory* (New York: Springer)
[18] Mahan G D 1981 *Many-Particle Physics* (New York: Plenum)
[19] Kadanoff L P and Baym G 1962 *Quantum Statistical Mechanics* (New York: Benjamin)
[20] Haug H and Jauho A-P 1996 *Quantum Kinetics in Transport and Optics of Semiconductors (Springer Series vol 123)* (New York: Springer)
[21] Geller Y L and Leburton J-P 1995 *Semicond. Sci. Technol.* **10** 1463
[22] Sulimov V B 1992 *Sov. Phys.–JETP* **74** 931
[23] Spivak B, Zhou F and Beal-Monod M T 1995 *Phys. Rev.* B **51** 13 226
[24] Langreth D C 1976 *Linear and Nonlinear Electron Transport in Solids* ed J T Devreese and E van Boren (New York: Plenum)
[25] Král P 1997 *J. Stat. Phys.* **86** 1337
[26] Adolph B *et al* 1996 *Phys. Rev.* B **53** 9797
[27] Binder R *et al* 1997 *Phys. Rev.* B **55** 5110
[28] Král P, Mele E J and Tománek D 2000 *Phys. Rev. Lett.* submitted
[29] Bir G L and Pikus G E 1974 *Symmetry and Strain-Induced Effects in Semiconductors* (New York: Wiley)
[30] Aversa C and Sipe J E 1995 *Phys. Rev.* B **52** 14 636